
Effect of Hydrostatic Pressure on Nonlinear Vibrating of Annular Circular Plate Coupled with Bounded Fluid

Amir Hossein Nasrollah Barati¹, Ali Asghar Jafari²,
Shahram Etemadi Haghighi^{1,*} and Adel Maghsoudpour¹

¹*Department of Mechanical Engineering, Science and Research Branch, Islamic Azad University, Tehran, Iran*

²*Department of Mechanical Engineering, K. N. Toosi University of Technology, Tehran, Iran*

E-mail: amirhoseinbarati@gmail.com; ajafari@kntu.ac.ir; setemadi@srbiau.ac.ir; a.maghsoudpour@srbiau.ac.ir

**Corresponding Author*

Received 09 February 2021; Accepted 01 April 2021;
Publication 19 May 2021

Abstract

The present study aims to evaluate the nonlinear vibration of an annular circular plate in contact with the fluid. Analysis of plate is based on first-order Shear Deformation Theory (FSDT) by considering of rotational inertial effects and transverse shear stresses. The governing equation of the oscillatory behavior of the fluid is determined by solving the Laplace equation and satisfying its boundary conditions. The nonlinear differential equations are solved based on the differential quadrature method and obtaining nonlinear natural frequency. In addition, the numerical results are presented for a sample plate, and the effect of some parameters such as aspect ratio, boundary conditions, fluid density, and fluid height are investigated. Finally, the results are compared with those of similar studies in the literature.

European Journal of Computational Mechanics, Vol. 29_4-6, 491-516.

doi: 10.13052/ejcm1779-7179.29468

© 2021 River Publishers

Keywords: Nonlinear vibration, annular circular plate, fluid pressure, differential quadrature method.

1 Introduction

In recent decades, some researchers have focused on studying structure behavior in contact with the fluid. Hydroelastic characteristics of plates in contact with fluid are important in various engineering applications such as micro-pumps, aerial structures, solar panels, marine structures, nuclear reactors and the like. Fluid-coupled vibrations causes failure and fatigue in the structure in some cases. Thus, controlling and even modifying this behavior is very important. A large body of research has been conducted on the vibration of the plate in contact with the fluid.

Kwak and Kim [1] investigated the vibration of a circular plate in contact with the ideal fluid in the axi-symmetrically state. The non-dimensional added virtual mass incremental factor for circular plates with simply supported, clamped and free edges determined by employing the integral transformation technique in conjunction with the dual integral equation method. Their study shown that the presence of fluid increases the inertia of the plate and a significant decrease occurs with dry state. Endo [2] studied the vibrational behavior of very large floating structures (VLFS) under the influence of moving load and waves by using the finite element method and indicated that waves increase the dynamic response of VLFS, the effect of which should be considered in designing these structures. Kozlovsky [3] examined the vibration of the plate in contact with the viscous fluid and indicated that the natural frequency of the plate decreases through contacting with the fluid. In another study. Askari et al. [4] reported the vibration of a circular plate immersed in finite fluid and used the semi-analytical method to solve the plate equations in simple edge support and free edge. Tariverdilo et al. [5] evaluated the free vibration of a circular plate in contact with a finite and incompressible fluid. They applied the Bessel-Fourier series and variation method to extract the natural frequencies of the plate and fluid, both of which yielded almost similar results. Finally, the effect of fluid depth on the added mass and natural frequencies of the plate in contact with the fluid was considered.

In another study, Allahverdizadeh et al. [6] developed a semi-analytical approach for nonlinear free and forced axisymmetric vibration of a thin circular functionally graded plate and reported that the free vibration frequencies are dependent on vibration amplitudes. In addition, the volume fraction index

has a significant influence on the nonlinear response specifications of the plate. Jeong [7] suggested an analytical method based on the finite Fourier-Bessel expansion and Rayleigh-Ritz methods and indicated that in-phase and out-of-phase two transverse vibration modes are alternately observed in the fluid-coupled system when the number of nodal circles increases for the fixed nodal diameter. Jeong and Kim [8] developed an analytical method to estimate the natural frequencies of a circular plate coupled with a compressible fluid by Rayleigh-Ritz and finite Fourier-Bessel series expansion methods. The results showed that the normalized natural frequencies decrease drastically when the offcenter distance approaches unity. In addition, Amabili studied [9] the free vibrations of circular and annular plates in contact with a finite fluid domain on one side, where the plates were placed in an annular (or circular) aperture of an infinite rigid wall and the fluid was assumed to be incompressible. Based on the results, natural frequencies decrease with the fluid depth when the fluid domain is limited by a free surface.

Shafiee et al. [10] developed free vibrations of a functionally graded elastic plate resting on Winkler elastic foundation in contact with a quiescent fluid and indicated that the natural frequencies of the fluid coupled system increase by increasing the material parameter. Further, the natural frequency of the plate increased when the elastic foundation stiffness increased. Canales and Mantari [11] considered an analytical solution for the free vibration analysis of thick rectangular composite plates in contact with a bounded fluid. They evaluated the classical boundary conditions using suitable functions in the Ritz series. Finally, the formulation analyzed thick plates with high accuracy, as observed from their comparison with a 3D finite element solution.

In another study, Bo [12] studied the vertical vibration of an elastic circular plate on fluid-saturated porous half space by a new analytical method. Also, the governing equations were developed by using the Hankel transform Techniques. In addition, Khorshidi et al. [13] focused on the free vibration response of a thin rectangular plate in contact with fluid by applying acoustic and modal tests. They considered the plate as one of the walls of a cubic tank containing fluid. They used a modal test to obtain plate natural frequencies and studied the effect of different parameters such as tank dimensions on the vibrational behavior of the plate in contact with the fluid. Soni et al. [14] proposed an analytical model for vibration analysis of partially cracked rectangular plates coupled with fluid. They modified the governing equations of plate based on the classical plate theory to consider the effect of linear crack. The effect of the fluid environment, which is characterized by inertia on the governing equations, was obtained based on the potential function of velocity

and Bernoulli's equation. Using multiple scales method, they examined the frequency response and peak amplitude of the crack structure. Soni et al. [15] proposed stability and dynamic analysis of partially cracked thin orthotropic microplates under a thermal environment. The crack was modeled by using appropriate crack compliance coefficients based on the simplified line spring model. They solved the cracking plate equation analytically to obtain the frequency and central deflection of plate.

By considering the above-mentioned studies, the nonlinear vibration of an annular circular plate in contact with a fluid has been less considered. Thus, the nonlinear free vibrations of an annular circular plate in contact with a fluid are analyzed using the first-order shear deformation theory. In addition, the effect of fluid presence on nonlinear natural frequency is evaluated. The equations of motion are obtained by the Hamilton principle and the dynamic pressure exerted by the fluid on the plate is obtained by solving the Laplace equation and applying boundary conditions in terms of the transverse displacement of the plate. In addition, the nonlinear differential equations are solved based on the DQM, and accordingly, the nonlinear natural frequency is determined. Further, the effect of parameters such as the dimensional ratio, boundary conditions, fluid density, and fluid height are investigated. Finally, the obtained results without considering the fluid are validated by comparing with those of the previous studies, and good convergence is observed.

2 Formulation

Consider an annular circular plate with the inner radius a , the outer radius b , and thickness h as illustrated in Figure 1.

The annular circular plate is considered to be in contact with fluid in a rigid cylindrical vessel at the $z = -h/2$, where d and H refer to radius and depth of the vessel, respectively. In addition, a_1 is considered as an internal fluid boundary.

Based on the first-order shear deformation plate theory, the displacement components are given as follows [16]:

$$\begin{aligned} u_r(r, \theta, z) &= u_0 + z\phi_r(r, \theta) \\ u_\theta(r, \theta, z) &= v_0 + z\phi_\theta(r, \theta) \\ u_z(r, \theta, z) &= w(r, \theta) \end{aligned} \quad (1)$$

Where z indicates the thickness coordinate, and u_r , u_θ and u_z are the displacement along the r , θ , and z axes, respectively. u_0 and v_0 are considered as

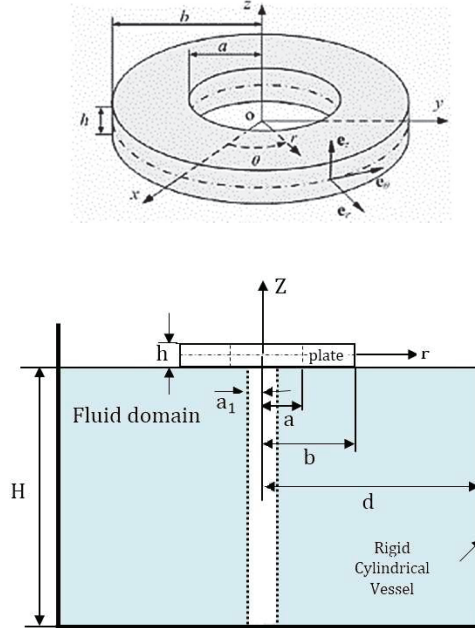


Figure 1 Circular plate in contact with the fluid with coordinate convection.

the displacement of mid-plane along the r and θ directions, respectively. Furthermore, ϕ_r and ϕ_θ show the rotational about the r and θ axes, respectively. Considering the nonlinear strain–displacement relationships, the strains are declared at an arbitrary point in the plate as follows [16]:

$$\begin{aligned}
 e_{rr} &= \frac{\partial u_r}{\partial r} + \frac{1}{2} \left(\frac{\partial u_z}{\partial r} \right)^2 = \frac{\partial u_0}{\partial r} + z \frac{\partial \phi_r}{\partial r} + \frac{1}{2} \left(\frac{\partial w}{\partial r} \right)^2 \\
 e_{\theta\theta} &= \frac{1}{r} \frac{\partial u_\theta}{\partial \theta} + \frac{u_r}{r} + \frac{1}{2r^2} \left(\frac{\partial u_z}{\partial \theta} \right)^2 = \frac{1}{r} \frac{\partial v_0}{\partial \theta} + \frac{u_0}{r} \\
 &\quad + \frac{z}{r} \left(\frac{\partial \phi_\theta}{\partial \theta} + \phi_r \right) + \frac{1}{2r^2} \left(\frac{\partial w}{\partial \theta} \right)^2 \\
 e_{r\theta} &= \frac{1}{2} \left(\frac{1}{r} \frac{\partial u_r}{\partial \theta} + \frac{\partial u_\theta}{\partial r} - \frac{u_\theta}{r} + \frac{1}{r} \frac{\partial u_z}{\partial r} \frac{\partial u_z}{\partial \theta} \right) \\
 &= \frac{1}{2} \left(z \left(\frac{1}{r} \frac{\partial \phi_r}{\partial \theta} + \frac{\partial \phi_\theta}{\partial r} - \frac{\phi_\theta}{r} \right) + \frac{1}{r} \frac{\partial u_0}{\partial \theta} + \frac{\partial v_0}{\partial r} - \frac{v_0}{r} + \frac{1}{r} \frac{\partial w}{\partial r} \frac{\partial w}{\partial \theta} \right)
 \end{aligned}$$

$$\begin{aligned}
e_{rz} &= \frac{1}{2} \left(\frac{\partial u_r}{\partial z} + \frac{\partial u_z}{\partial r} \right) = \frac{1}{2} \left(\phi_r + \frac{\partial w}{\partial r} \right) \\
e_{\theta z} &= \frac{1}{2} \left(\frac{\partial u_\theta}{\partial z} + \frac{1}{r} \frac{\partial u_z}{\partial \theta} \right) = \frac{1}{2} \left(\phi_\theta + \frac{1}{r} \frac{\partial w}{\partial \theta} \right)
\end{aligned} \quad (2)$$

2.1 Hamilton's Principle

The Hamilton's principle is used for obtaining the equations of motion of the circular plate [17]:

$$\delta \int_{t_1}^{t_2} (T - U + W_{n.c}) dt = 0 \quad (3)$$

Where T , U , and $W_{n.c}$ indicate kinetic energy, strain energy, and work done by external loads, respectively.

Further, the kinetic energy of the plate is defined as Equation (4) [17]:

$$T = \frac{1}{2} \iiint \rho(r, \theta, z) (\dot{u}_r^2 + \dot{u}_\theta^2 + \dot{u}_z^2) dV \quad (4)$$

By substituting Equation (1) into Equation (4), the kinetic energy is calculated as follows:

$$\begin{aligned}
T &= \frac{1}{2} \int_{-\frac{h}{2}}^{\frac{h}{2}} \int_0^{2\pi} \int_a^b \rho(r, \theta, z) (\dot{u}_0^2 + z^2 \dot{\phi}_r^2 + 2\dot{u}_0 z \dot{\phi}_r \\
&\quad + \dot{v}_0^2 + z^2 \dot{\phi}_\theta^2 + 2\dot{v}_0 z \dot{\phi}_\theta + \dot{w}^2) r dr d\theta dz
\end{aligned} \quad (5)$$

By integrating Equation (5) with respect to the thickness direction, the variations of kinetic energy are determined by using the variational principle for equations and integration terms by parts as follows:

$$\begin{aligned}
\int_{t_1}^{t_2} \delta T dt &= \frac{1}{2} \int_{t_1}^{t_2} \int_0^{2\pi} \int_a^b -(2\rho_0 \ddot{u}_0 \delta u_0 + 2\rho_2 \ddot{\phi}_r \delta \phi_r \\
&\quad + 2\rho_1 \ddot{\phi}_r \delta u_0 + 2\rho_1 \ddot{u}_0 \delta \phi_r + 2\rho_0 \ddot{v}_0 \delta v_0 + 2\rho_2 \ddot{\phi}_\theta \delta \phi_\theta \\
&\quad + 2\rho_1 \ddot{\phi}_\theta \delta v_0 + 2\rho_1 \ddot{v}_0 \delta \phi_\theta + 2\rho_0 \ddot{w} \delta w) r dr d\theta
\end{aligned} \quad (6)$$

Where ρ_0 , ρ_1 , and ρ_2 indicate the inertia terms defined as follows.

$$(\rho_0, \rho_1, \rho_2) = \int_{-\frac{h}{2}}^{\frac{h}{2}} (1, z, z^2) \rho(r, \theta, z) dz \quad (7)$$

The strain energy stored in the plate is given as Equation (8) [17]:

$$U = \frac{1}{2} \iiint \sigma_{ij} e_{ij} dv = \frac{1}{2} \int_{-\frac{h}{2}}^{\frac{h}{2}} \int_0^{2\pi} \int_a^b (\sigma_{rr} e_{rr} + \sigma_{\theta\theta} e_{\theta\theta} + 2\sigma_{r\theta} e_{r\theta} + 2\sigma_{rz} e_{rz} + 2\sigma_{\theta z} e_{\theta z}) r dr d\theta dz \quad (8)$$

By substituting Equation (2) into Equation (8), Equation (9) is obtained through integrating with respect to the thickness direction, applying the variation method [17], and integrating the terms by parts:

$$\begin{aligned} dU = & \int_0^{2\pi} \int_a^b \{ \delta\phi_r (-rM_{rr})_{,r} + M_{\theta\theta} - (M_{r\theta})_{,\theta} + r\phi_r \\ & + \delta U_0 (-rN_{rr})_{,r} - N_{\theta\theta} - (N_{r\theta})_{,\theta} \\ & + \delta V_0 (-N_{\theta\theta})_{,\theta} - (rN_{r\theta})_{,r} - N_{r\theta} \\ & + \delta W (-rQ_r)_{,r} - Q_{\theta,\theta} \\ & + \delta\phi_\theta (-rM_{r\theta})_{,r} - M_{r\theta} + rQ_\theta - M_{\theta\theta,\theta} \} dr d\theta \end{aligned} \quad (9)$$

where M_{rr} , $M_{\theta\theta}$, and $M_{r\theta}$ are considered as bending moment resultants, N_{rr} , $N_{\theta\theta}$ and $N_{r\theta}$ represent membrane force resultants, and Q_r and Q_θ are shear force resultants, which are defined as follows.

$$\begin{aligned} (M_{rr}, M_{\theta\theta}, M_{r\theta}) &= \int_{-\frac{h}{2}}^{\frac{h}{2}} (\sigma_{rr}, \sigma_{\theta\theta}, \sigma_{r\theta}) z dz \\ (N_{rr}, N_{\theta\theta}, N_{r\theta}) &= \int_{-\frac{h}{2}}^{\frac{h}{2}} (\sigma_{rr}, \sigma_{\theta\theta}, \sigma_{r\theta}) dz \\ (Q_r, Q_\theta) &= \int_{-\frac{h}{2}}^{\frac{h}{2}} (\sigma_{rz}, \sigma_{\theta z}) dz \end{aligned} \quad (10)$$

Also, the variations in the work of the non-conservative forces are as follows:

$$\delta w_{n.c} = \int_0^{2\pi} \int_a^b (-p(r, \theta, t)) \delta w r dr d\theta \quad (11)$$

Where $p(r, \theta, t)$ is the dynamic pressure applied by the fluid.

In addition, the governing differential equations of the plate can be obtained as substituting Equations (6), (9), and (11) into Equation (3) and using the variational principle:

$$\begin{aligned}
\frac{1}{r}(N_{rr} - N_{\theta\theta}) + \frac{1}{r}N_{r\theta,\theta} + N_{rr,r} &= \rho_0\ddot{u}_0 + \rho_1\ddot{\phi}_r \\
\frac{2}{r}N_{r\theta} + N_{r\theta,r} + \frac{1}{r}N_{\theta\theta,\theta} &= \rho_0\ddot{v}_0 + \rho_1\ddot{\phi}_\theta \\
\frac{1}{r}(M_{rr} - M_{\theta\theta}) + M_{rr,r} + \frac{1}{r}M_{r\theta,\theta} - Q_r &= \rho_2\ddot{\phi}_r + \rho_1\ddot{u}_0 \\
\frac{2}{r}M_{r\theta} + M_{r\theta,r} + \frac{1}{r}M_{\theta\theta,\theta} - Q_\theta &= \rho_2\ddot{\phi}_\theta + \rho_1\ddot{v}_0 \\
\frac{1}{r}Q_r + Q_{r,r} + \frac{1}{r}Q_{\theta,\theta} + \frac{1}{r}(rN_{rr}w_{,r})_{,r} + \frac{1}{r^2}(N_{\theta\theta}w_{,\theta})_{,\theta} \\
+ \frac{1}{r}(N_{r\theta}w_{,\theta})_{,r} + \frac{1}{r}(N_{r\theta}w_{,r})_{,\theta} &= \rho_0\ddot{w} - p
\end{aligned} \tag{12}$$

3 Fluid Pressure

The following assumptions are considered for the dynamic model behavior in order to determine the fluid pressure.

1. The desired fluid is ideally considered. Therefore, a potential function can be considered for it.
2. Fluid displacements and velocities are assumed to be small and the fluid behavior is considered to be linear.
3. The initial condition of the fluid is considered as zero.
4. Fluid pressure formulation is based on the velocity potential function.
5. The fluid is considered incompressible, non-viscous, and non-rotating.

Given the above conditions for the fluid in contact, the velocity potential function Φ must satisfy the Laplace equation in the fluid amplitude. The form of the equation in cylindrical coordinates is as follows [18].

$$\nabla^2\Phi(r, \theta, z, t) = \frac{\partial^2\Phi}{\partial r^2} + \frac{1}{r}\frac{\partial\Phi}{\partial r} + \frac{1}{r^2}\frac{\partial^2\Phi}{\partial\theta^2} + \frac{\partial^2\Phi}{\partial z^2} = 0 \tag{13}$$

Also, the boundary conditions of the problem are as follows.

$$(v_r)_{r=a_1,d} = 0 \rightarrow \left(\frac{\partial\Phi}{\partial r}\right)_{r=a_1} = \left(\frac{\partial\Phi}{\partial r}\right)_{r=d} = 0$$

$$(v_z)_{z=-\frac{h}{2}-H} = 0 \rightarrow \left(\frac{\partial\Phi}{\partial z}\right)_{z=-\frac{h}{2}-H} = 0.$$

$$(v_z)_{fluid} = (v_z)_{plate} \text{ in contact surface} \rightarrow \left(\frac{\partial\Phi}{\partial z}\right)_{z=-\frac{h}{2}} = \frac{\partial w}{\partial t} \quad (14)$$

Using the Bernoulli equation, irrespective of the non-rotational expression, the fluid pressure at the fluid-structural contact surface is considered as follows [4].

$$p = p|_{z=-\frac{h}{2}} = -\rho_f \frac{\partial\Phi}{\partial t} \Big|_{z=-\frac{h}{2}} \quad (15)$$

In the above equation, ρ_f shows the density of the fluid in unit volume. Equation (16) is obtained by using the method of separating variables and applying boundary conditions, and placing the potential function in relation to the dynamic pressure applied by the fluid on the plate as follows.

$$p(r, \theta, t) = -\rho_f \sum_{m=1}^{\infty} \sum_{n=1}^{\infty} \frac{\coth(\eta_{mn}H)}{\eta_{mn}} \ddot{w}(r, \theta, t) \quad (16)$$

Furthermore, η_{mn} is determined as follows.

$$J'_{\beta_m}(\eta a_1) Y'_{\beta_m}(\eta d) - J'_{\beta_m}(\eta d) Y'_{\beta_m}(\eta a_1) = 0 \quad (17)$$

Also, J and Y are the polar Bessel function of the first and second types and $\beta_m = n$.

4 Numerical Methods

In this study, the Differential Quadrature Method (DQM) is used as a fast and accurate method for the numerical solution of governing differential equations. Using fewer nodes and reducing computational time and cost are considered as the main advantages of using DQM compared to the finite element method. According to DQM, the solution domain is discretized into N discrete grid points. In this method, the partial derivative of a function is approximately expressed with respect to the space variable at a given discrete point by a sum of the weighted linear functions and function values at all discrete points. Thus, in each point, the derivative is a linear set of weight coefficients and the function values are presented along the directions of a coordinate axis in the same point and other points of the domain. Then, the

n th order partial derivative of a given function $g(r, \theta)$ with respect to r and the s th order partial derivative with respect to θ are established in each point of the grid (r_i, θ_j) as follows.

$$\begin{aligned} \frac{\partial^n g}{\partial r^n} \Big|_{(r,\theta)=(r_i,\theta_j)} &= \sum_{k=1}^{N_r} B_{ik}^n g_{kj} \\ \frac{\partial^s g}{\partial \theta^s} \Big|_{(r,\theta)=(r_i,\theta_j)} &= \sum_{k=1}^{N_\theta} C_{jk}^s g_{ik} \\ i &= 1, \dots, N_r \quad j = 1, \dots, N_\theta \\ \frac{\partial^{(n+s)} g}{\partial r^n \partial \theta^s} \Big|_{(r,\theta)=(r_i,\theta_j)} &= \sum_{k=1}^{N_r} B_{ik}^n \sum_{l=1}^{N_\theta} C_{jl}^s g_{kl} \end{aligned} \quad (18)$$

Where g_{ij} denotes $g(r_i, \theta_j)$ [19], B_{ik}^n and C_{jk}^s are considered as the weight coefficients in the r and θ directions, respectively, which refers to test functions. It is worth noting that the behavior of this method is related to the selection of weight coefficients. In this study, the polynomial test functions are used for weight coefficients along a direction, which is defined as follows [19]:

$$\begin{aligned} B_{ik}^{(1)} &= \frac{\prod(r_i)}{(r_i - r_k) \prod(r_k)} i, \quad k = 1, \dots, N_r \text{ \& } k \neq i \\ \prod(r_i) &= \prod_{m=1, m \neq i}^{N_r} (r_i - r_m), \quad \prod(r_k) = \prod_{m=1, m \neq k}^{N_r} (r_k - r_m) \\ B_{ik}^{(n)} &= n \left(B_{ii}^{(n-1)} B_{ik}^{(1)} - \frac{B_{ik}^{(n-1)}}{r_i - r_k} \right); \text{ for } (i, k = 1, \dots, N_r), \\ & \quad k \neq i, 2 \leq n \leq N_r - 1 \\ B_{ii}^{(n)} &= - \sum_{m=1, m \neq i}^{N_r} B_{im}^{(n)}; \text{ for } i = 1, \dots, N_r, 1 \leq n \leq N_r - 1 \end{aligned} \quad (19)$$

In numerical computations, Chebyshev–Gauss–Lobatto quadrature points are used as the location relationships of grid points for the annular circular

plate in r and θ directions, respectively, which are expressed as follows [19]:

$$r_i = \left(b + \frac{1}{2} \left[1 - \cos \left(\frac{(i-1)\pi}{N_R - 1} \right) \right] (a - b) \right) \quad i = 1, 2, \dots, N_R \quad (20a)$$

$$\theta_j = \frac{\alpha}{2} \left[1 - \cos \left(\frac{(j-1)\pi}{N_\theta - 1} \right) \right] \quad j = 1, 2, \dots, N_\theta \quad (20b)$$

Further, the annular circular plate equations of motion yield as:

$$\begin{aligned} \rho_0 \ddot{u}_0 + \rho_1 \ddot{\phi}_r = & A_1 \left(\frac{\partial^2 u_0}{\partial r^2} + \frac{1}{r} \frac{\partial u_0}{\partial r} - \frac{1}{r^2} \frac{\partial v_0}{\partial \theta} - \frac{u_0}{r^2} + \frac{1}{r} \frac{\partial^2 v_0}{\partial r \partial \theta} \right. \\ & \left. + \frac{\partial w}{\partial r} \frac{\partial^2 w}{\partial r^2} - \frac{1}{r^3} \left(\frac{\partial w}{\partial \theta} \right)^2 + \frac{1}{r^2} \frac{\partial w}{\partial \theta} \frac{\partial^2 w}{\partial r \partial \theta} \right) \\ & + A_2 \left(\frac{1}{r^2} \frac{\partial^2 u_0}{\partial \theta^2} - \frac{1}{r^2} \frac{\partial v_0}{\partial \theta} - \frac{1}{r} \frac{\partial^2 v_0}{\partial r \partial \theta} + \frac{1}{r^3} \left(\frac{\partial w}{\partial \theta} \right)^2 \right. \\ & \left. + \frac{1}{r} \left(\frac{\partial w}{\partial r} \right)^2 - \frac{1}{r^2} \frac{\partial w}{\partial \theta} \frac{\partial^2 w}{\partial r \partial \theta} + \frac{1}{r^2} \frac{\partial w}{\partial \theta} \frac{\partial^2 w}{\partial \theta^2} \right) \end{aligned} \quad (21a)$$

$$\begin{aligned} \rho_0 \ddot{v}_0 + \rho_1 \ddot{\phi}_\theta = & A_1 \left(\frac{1}{r^2} \frac{\partial^2 v_0}{\partial \theta^2} + \frac{1}{r^2} \frac{\partial u_0}{\partial \theta} + \frac{1}{r} \frac{\partial^2 u_0}{\partial r \partial \theta} + \frac{1}{r^3} \frac{\partial w}{\partial \theta} \frac{\partial^2 w}{\partial \theta^2} \right. \\ & \left. + \frac{1}{r} \frac{\partial w}{\partial r} \frac{\partial^2 w}{\partial r \partial \theta} \right) \\ & + A_2 \left(\frac{1}{r^2} \frac{\partial u_0}{\partial \theta} - \frac{1}{r} \frac{\partial^2 u_0}{\partial r \partial \theta} + \frac{\partial^2 v_0}{\partial r^2} - \frac{v_0}{r^2} + \frac{1}{r} \frac{\partial v_0}{\partial r} \right. \\ & \left. + \frac{1}{r^2} \frac{\partial w}{\partial r} \frac{\partial w}{\partial \theta} - \frac{1}{r} \frac{\partial w}{\partial r} \frac{\partial^2 w}{\partial r \partial \theta} + \frac{1}{r} \frac{\partial w}{\partial \theta} \frac{\partial^2 w}{\partial r^2} \right) \end{aligned} \quad (21b)$$

$$\begin{aligned} \rho_2 \ddot{\phi}_r + \rho_1 \ddot{u}_0 = & A_3 \left(\frac{\partial^2 \phi_r}{\partial r^2} + \frac{1}{r} \frac{\partial \phi_r}{\partial r} - \frac{1}{r^2} \frac{\partial \phi_\theta}{\partial \theta} - \frac{\phi_r}{r^2} + \frac{1}{r} \frac{\partial^2 \phi_\theta}{\partial r \partial \theta} \right) \\ & + A_4 \left(\frac{1}{r^2} \frac{\partial^2 \phi_r}{\partial \theta^2} - \frac{1}{r^2} \frac{\partial \phi_\theta}{\partial \theta} - \frac{1}{r} \frac{\partial^2 \phi_\theta}{\partial r \partial \theta} \right) - A_2 \left(\phi_r + \frac{\partial w}{\partial r} \right) \end{aligned} \quad (21c)$$

$$\begin{aligned} \rho_2 \ddot{\phi}_\theta + \rho_1 \ddot{v}_0 = & A_3 \left(\frac{1}{r^2} \frac{\partial^2 \phi_\theta}{\partial \theta^2} + \frac{1}{r^2} \frac{\partial \phi_r}{\partial \theta} + \frac{1}{r} \frac{\partial^2 \phi_r}{\partial r \partial \theta} \right) \\ & + A_4 \left(\frac{1}{r^2} \frac{\partial \phi_r}{\partial \theta} - \frac{1}{r} \frac{\partial^2 \phi_r}{\partial r \partial \theta} + \frac{\partial^2 \phi_\theta}{\partial r^2} - \frac{\phi_\theta}{r^2} + \frac{1}{r} \frac{\partial \phi_\theta}{\partial r} \right) \\ & - A_2 \left(\phi_\theta + \frac{1}{r} \frac{\partial w}{\partial \theta} \right) \end{aligned} \quad (21d)$$

$$\begin{aligned} \rho_0 \ddot{w} + \rho_f \sum_{m=1}^{\infty} \sum_{n=1}^{\infty} \frac{\coth(\eta_{mn} H)}{\eta_{mn}} \ddot{w}(r, \theta, t) \\ = A_2 \left(\frac{\partial \phi_r}{\partial r} + \frac{\phi_r}{r} + \frac{1}{r} \frac{\partial \phi_\theta}{\partial \theta} + \frac{\partial^2 w}{\partial r^2} + \frac{1}{r} \frac{\partial w}{\partial r} + \frac{1}{r^2} \frac{\partial^2 w}{\partial \theta^2} \right) \\ + N_{rr} \frac{\partial^2 w}{\partial r^2} + 2N_{r\theta} \left(\frac{1}{r} \frac{\partial^2 w}{\partial r \partial \theta} - \frac{1}{r^2} \frac{\partial w}{\partial \theta} \right) \\ + N_{\theta\theta} \left(\frac{1}{r^2} \frac{\partial^2 w}{\partial \theta^2} + \frac{1}{r} \frac{\partial w}{\partial r} \right) \end{aligned} \quad (21e)$$

Where the coefficient A_1, A_2, A_3, A_4 are defined as follows

$$\begin{aligned} A_1 = \frac{1}{1 - \nu^2} \int_{-\frac{h}{2}}^{\frac{h}{2}} E dz, \quad A_2 = \frac{1}{2(1 + \nu)} \int_{-\frac{h}{2}}^{\frac{h}{2}} E dz \\ A_3 = \frac{1}{1 - \nu^2} \int_{-\frac{h}{2}}^{\frac{h}{2}} E z^2 dz, \quad A_4 = \frac{1}{2(1 + \nu)} \int_{-\frac{h}{2}}^{\frac{h}{2}} E z^2 dz \end{aligned} \quad (22)$$

In this paper, four types of boundary conditions are considered as follows.

Clamped-clamped

$$r = a, b \quad u_0 = v_0 = w = \phi_r = \phi_\theta = 0 \quad (23a)$$

Simple-simple

$$r = a, b \quad u_0 = v_0 = w = \phi_\theta = M_{rr} = 0 \quad (23b)$$

Clamped-simple

$$\begin{aligned} r = a, b \quad u_0 = v_0 = w = \phi_r = \phi_\theta = 0 \\ r = a, b \quad u_0 = v_0 = w = \phi_\theta = M_{rr} = 0 \end{aligned} \quad (23c)$$

Simple-clamped

$$\begin{aligned} r = a, b \quad u_0 = v_0 = w = \phi_\theta = M_{rr} = 0 \\ r = a, b \quad u_0 = v_0 = w = \phi_r = \phi_\theta = 0 \end{aligned} \tag{23d}$$

To study the flexural vibration of thin plates, u and v are considerably smaller than the transverse displacement and the effects of in-plane inertia can be neglected [20]. Consequently, the in-plane degrees of freedom can be eliminated from the final eigenvalue system of equations, which causes a considerable reduction in the computational efforts, especially for nonlinear vibration analysis of circular plates, which has an iterative procedure solution. To eliminate the in-plane degrees of freedom, one can write the in-plane forces at all the domain grid points in the matrix form as follows.

$$\begin{Bmatrix} N_{rr} \\ N_{\theta\theta} \\ N_{r\theta} \end{Bmatrix} = [C_{dd}] \begin{Bmatrix} \{u_0\}_d \\ \{v_0\}_d \end{Bmatrix} + \{F(w)\} \tag{24}$$

Where $[C_{dd}]$ indicates the coefficient matrix, $\{F(w)\}$ shows a quadratic function of transverse displacement w obtained from the discretized form of the in-plane forces. $\{u_0\}_d$ and $\{v_0\}_d$ are considered as the vectors of the in-plane displacements at the domain grid points. On the other hand, neglecting the in-plane inertia forces, the discretized form of the in-plane equations of motion (21a)–(21b) can be rearranged in the matrix form as follows.

$$[S_{uu}] \begin{Bmatrix} \{u_0\}_d \\ \{v_0\}_d \end{Bmatrix} + \{G(w)\} = \{0\} \tag{25}$$

Where the vector $\{G(w)\}$ indicates a quadratic function of transverse displacement and $[S_{uu}]$ shows the in-plane stiffness matrix. Using Equation (25), the constitutive Equation (24) at the domain grid points is written as follows.

$$\begin{Bmatrix} \{N_{rr}\} \\ \{N_{\theta\theta}\} \\ \{N_{r\theta}\} \end{Bmatrix} = -[C_{dd}][S_{uu}]^{-1}\{G(w)\} + \{F(w)\} = \{N(w^2)\} \tag{26}$$

Where the vector $\{N(w^2)\}$ is a quadratic function of the transverse displacement w . The following equation is obtained by substituting

Equation (26) into the DQ discretized form of Equation (18e)

$$\begin{aligned} & \begin{bmatrix} [M_{ww}] & [0] \\ [0] & [M_{\phi\phi}] \end{bmatrix} \begin{Bmatrix} \{\ddot{w}\}_d \\ \{\ddot{\phi}\}_d \end{Bmatrix} + \begin{bmatrix} [K_{ww}(w)] & [K_{w\phi}] \\ [K_{\phi w}] & [K_{\phi\phi}] \end{bmatrix} \begin{Bmatrix} \{w\}_d \\ \{\phi\}_d \end{Bmatrix} \\ & + \begin{bmatrix} [K_{wb}] \\ [K_{\phi b}] \end{bmatrix} \{U\}_b = \{0\} \end{aligned} \quad (27)$$

Further, $[K_{ww}(w)]$ is the sum of linear and nonlinear stiffness matrix, which is a cubic function of transverse displacement vector $\{w\}$. $[K_{w\phi}]$, $[K_{\phi w}]$ and $[K_{\phi\phi}]$ are linear stiffness matrices which represent the role of domain degrees of freedom in the equations of motion. $[K_{wb}]$ and $[K_{\phi b}]$ indicate linear stiffness matrices, which show the interaction between boundary degrees of freedom and equations of motion. Furthermore, $[M_{ww}]$ and $[M_{\phi\phi}]$ are considered as the mass matrices and $\{\phi\} = \begin{Bmatrix} \{\phi_r\} \\ \{\phi_\theta\} \end{Bmatrix}$. Also, the symbol of $(\ddot{\cdot})$ indicates the second derivative with respect to time. The DQ discretized form of boundary conditions is written in the matrix form as follows.

$$[[K_{bb}] \ [K_{bd}]] \begin{Bmatrix} \{U\}_b \\ \{\phi\}_d \end{Bmatrix} = \{0\} \quad (28)$$

Where $[K_{bb}]$ and $[K_{bd}]$ show the linear boundary stiffness matrices. Using Equation (28) for eliminating the boundary degrees of freedom of Equation (27) leads to a system of the differential equations in temporal domain as follows.

$$\begin{bmatrix} [M_{ww}] & [0] \\ [0] & [M_{\phi\phi}] \end{bmatrix} \begin{Bmatrix} \{\ddot{w}\}_d \\ \{\ddot{\phi}\}_d \end{Bmatrix} + \begin{bmatrix} [K_{ww}(w)] & [K_{w\phi}] \\ [K_{\phi w}] & [K_{\phi\phi}] \end{bmatrix} \begin{Bmatrix} \{w\}_d \\ \{\phi\}_d \end{Bmatrix} = \{0\} \quad (29)$$

Where $[K_{w\phi}]$ and $[K_{\phi\phi}]$ are linear stiffness matrices which are given as follows.

$$\begin{aligned} [\bar{K}_{w\phi}] &= [K_{w\phi}] - [K_{wb}][K_{bb}]^{-1}[K_{bd}], \\ [\bar{K}_{\phi\phi}] &= [K_{\phi\phi}] - [K_{\phi b}][K_{bb}]^{-1}[K_{bd}] \end{aligned} \quad (30)$$

In the present analysis, the solution algorithms are based on the harmonic balance method [17]. Regarding the harmonic balance method, it is assumed that the nonlinear system undergoes a harmonic motion, which is reasonable

in many cases, particularly for moderate vibration amplitudes. This simplification allows one to obtain a compact frequency domain model, which provides very useful information. The domain degrees of freedom are written by using this method.

$$\begin{Bmatrix} \{w\}_d \\ \{\phi\}_d \end{Bmatrix} = \begin{Bmatrix} \{W\} \\ \{\phi\} \end{Bmatrix} \cos(\omega t) \quad (31)$$

Where $\begin{Bmatrix} \{W\} \\ \{\phi\} \end{Bmatrix}$ is the vector of generalized amplitudes of the harmonic motions. Inserting Equation (31) into Equation (29), as well as the use of the harmonic balance method results in allowing frequency-domain equations of motion.

$$-\omega^2 \begin{bmatrix} [M_{ww}] & [0] \\ [0] & [M_{\phi\phi}] \end{bmatrix} \begin{Bmatrix} \{w\}_d \\ \{\phi\}_d \end{Bmatrix} + \begin{bmatrix} [K_{ww}(w)] & [K_{w\phi}] \\ [K_{\phi w}] & [K_{\phi\phi}] \end{bmatrix} \begin{Bmatrix} \{w\}_d \\ \{\phi\}_d \end{Bmatrix} = \{0\} \quad (32)$$

Where $[K_{ww}(w)] = [K^L_{ww}] + 3/4[K^{NL}_{ww}(w)]$. Also, $[K^{NL}_{ww}(w)]$ are the linear and nonlinear stiffness matrices, respectively. An iterative method should be used to solve the system of nonlinear eigenvalue (Equation (32)). In the iterate procedure, the linear problem is first solved by vanishing the nonlinear terms in this equation. Furthermore, the linear eigenvectors are used to obtain the nonlinear coefficients. The eigenvalue problem is solved again to determine the nonlinear eigenvalues and eigenvectors. The iterative procedure continues until two frequencies obtained from subsequent iterations can satisfy the following equation.

$$\left| \frac{\omega^{K+1} - \omega^k}{\omega^k} \right| \leq 0.001 \quad (33)$$

5 Numerical Results and Discussion

In this section the parameters affecting the natural nonlinear frequency of an annular circular plate in contact with a fluid is investigated. In addition, an annular circular plate of aluminum with the characteristics is considered as $\rho = 2707 \text{ kg/m}^3$, $E = 70 \text{ GPa}$, $\nu = 0.3$, and $\rho_f = 1000 \text{ kg/m}^3$. As shown in Table 1, for validation in a linear mode without considering nonlinear strain term, the non-dimensional natural frequencies of the clamped annular plate is considered as $\beta = b^2\omega\sqrt{h\rho/D}$, where different thickness ratios were

Table 1 Comparison of the dimensionless natural frequencies of the clamped annular plate for different thickness with Ref. [21]

a/b	h/b	Method	β_1	%Error	β_2	%Error	β_3	%Error	β_4	%Error
0.1	0.05	Ref. [21]	26.546	0.03%	71.232	0.01%	135.245	0.01%	215.114	0.01%
		present	26.538		71.228		135.244		215.112	
	0.1	Ref. [21]	24.634	0.01%	62.146	0.01%	111.127	0.01%	167.166	0.01%
		present	24.631		62.144		111.124		167.161	
	0.2	Ref. [21]	19.852	0.02%	44.922	0.01%	74.869	0.01%	106.815	0.01%
		present	19.847		44.918		74.862		106.812	
0.3	0.05	Ref. [21]	43.604	0.01%	115.272	0.01%	214.625	0.01%	334.708	0.01%
		present	43.602		115.270		214.621		334.706	
	0.1	Ref. [21]	39.395	0.01%	95.598	0.01%	165.267	0.01%	242.176	0.01%
		present	39.390		95.595		165.260		242.171	
	0.2	Ref. [21]	30.046	0.01%	64.239	0.01%	104.095	0.01%	145.236	0.01%
		present	30.041		64.234		104.093		145.235	

compared with the results given by [21]. Based on the results, an excellent agreement was observed for all of the cases.

Further, the results reported from the [21] are used (dry plate) for validating the results of nonlinear frequency. Figure 2 displays the results of an annular circular plate with the aspect ratios of $a/b = 0.3$ and $h/b = 0.1$ in terms of non-dimensional transverse displacement amplitude of the plate (w_{max}/h) for clamped boundary conditions. The results are consistent with those of [21].

The natural dimensionless nonlinear frequency is defined as $\bar{\omega}_{NL} = \omega_{NL} b^2 \sqrt{h\rho/D}$. Also, the nonlinear natural frequency of a plate in contact with a fluid depends on some parameters such as dimensional ratio, fluid characteristics, and non-dimensional transverse displacement amplitude of the plate (w_{max}/h). As shown in Figure 3, the w_{max}/h effect is evaluated for the four state conditions of the boundary conditions, which indicates that the dimensionless ratio of frequency (nonlinear natural frequency to linear natural frequency) increases by increasing w_{max}/h .

For example, CC and SS modes are used for evaluating different factors on nonlinear natural frequency. Now, the results are provided for $a/b = 0.1, 0.2, 0.3$.

As illustrated in Figures 4 and 5, the non-dimensional natural frequency of the circular plate in contact with fluid increases by increasing a/b

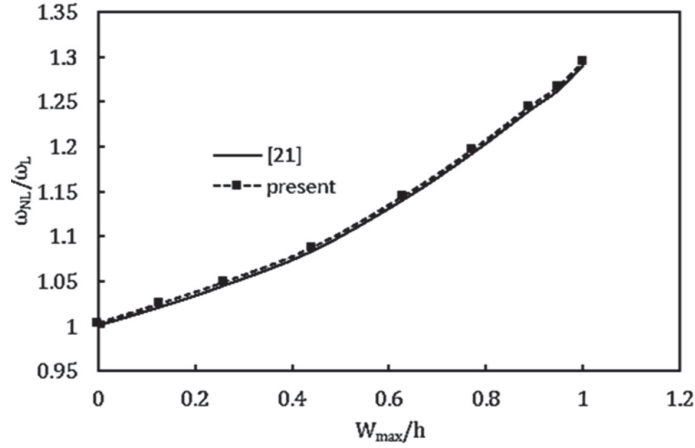


Figure 2 Dependency of the ratio of nonlinear to linear frequencies of the clamped annular plate with dimensionless vibration amplitudes for the first axisymmetric mode shapes.

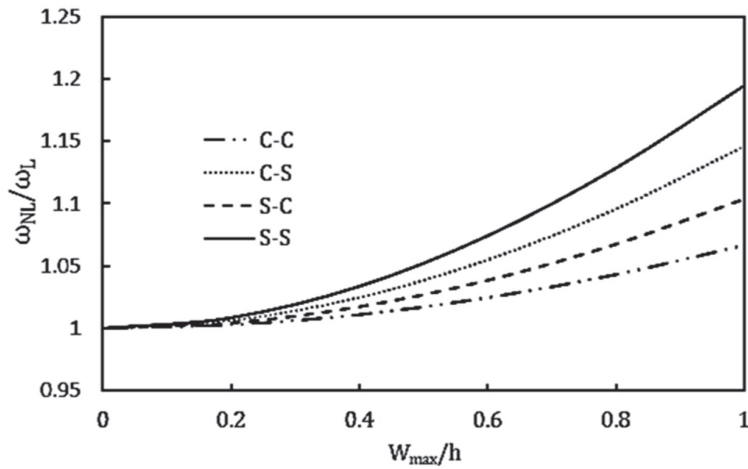


Figure 3 Frequency ratio (nonlinear frequency to linear frequency) for four different boundary modes.

(decreasing plate width). Further, a decrease in the width of the plate leads to a decrease in its inertia and stiffness increases which causes the frequency to increase.

Figure 6 shows the CC and SS modes examining the effect of the h/b aspect ratio on the dimensionless nonlinear natural frequency. The results of $h/b = 0.05, 0.1$ are presented as follows.

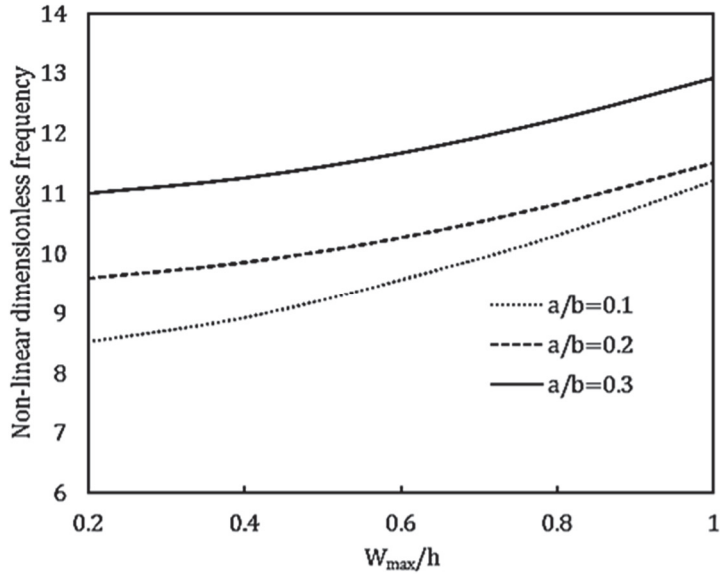


Figure 4 The effects of dimensional ratio changes a/b on the dimensionless nonlinear natural frequency of an annular circular plate in contact with a fluid for CC boundary conditions.

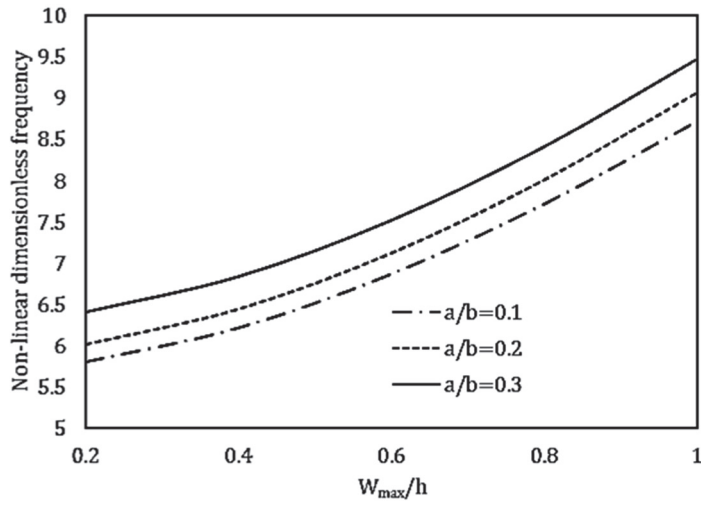


Figure 5 The effects of dimensional ratio changes a/b on the dimensionless nonlinear natural frequency of an annular circular plate in contact with a fluid for SS boundary conditions.

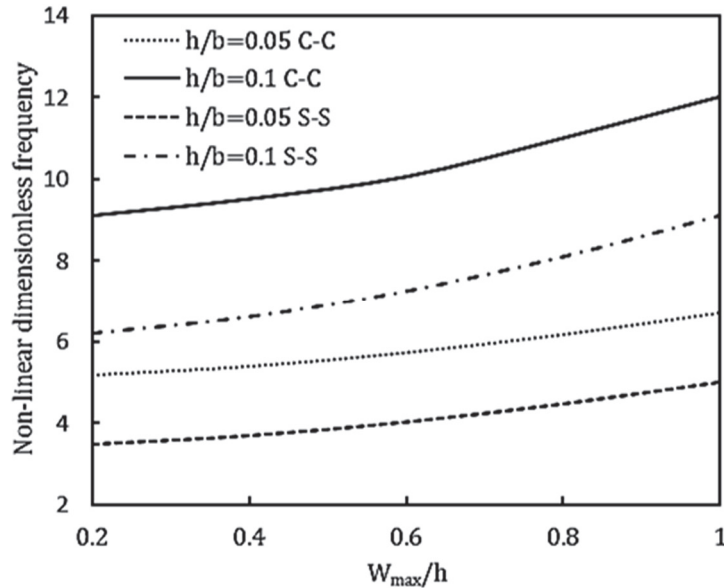


Figure 6 The effects of dimensional ratio changes h/b on the dimensionless nonlinear natural frequency of an annular circular plate in contact with a fluid for four boundary conditions.

As shown, the dimensionless natural nonlinear frequency of the circular plate in contact with the fluid increases by increasing h/b (thickening of the plate). In addition, an increase in the thickness of the plate leads to an increase in mass and stiffness. However, the ratio of increasing stiffness is higher than that of inertia, leading to an increase in the natural frequency.

Figures 7 and 8 display the effects of fluid density change on the dimensionless nonlinear natural frequency of circular plate in CC and SS modes.

As shown in Figures 7 and 8, it is expected that the dimensionless nonlinear natural frequency of the plate could decrease by increasing fluid density (heavier fluid).

The fluid behaves like the mass added to the plate since it is assumed to be non-viscous and has only inertia. Therefore, as the density of the fluid increases, the mass added to the plate increases and the frequency decreases.

In addition, as displayed in Figures 7 and 8, the dimensionless natural nonlinear frequency of the plate decreases with a very steep slope in the density range of 0–0.3, which indicates that the presence of fluid reduces the nonlinear natural frequency significantly.

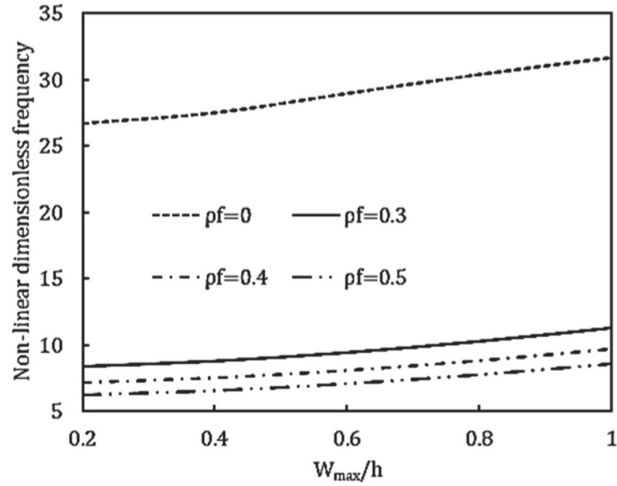


Figure 7 The effect of fluid density on the dimensionless nonlinear natural frequency of an annular circular plate in contact with a fluid for CC boundary conditions.

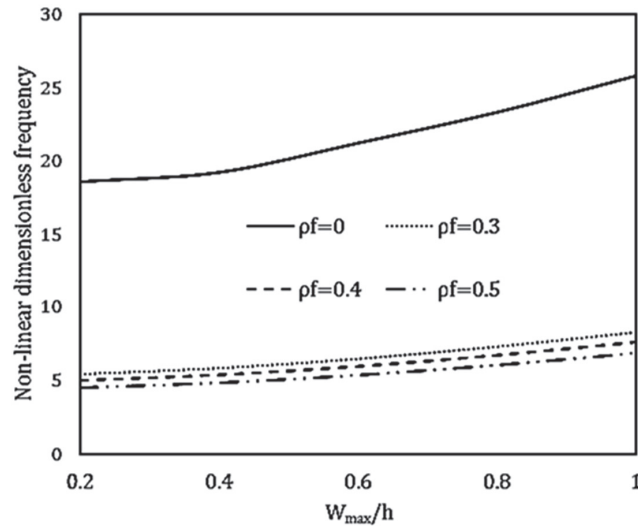


Figure 8 The effect of fluid density on the dimensionless nonlinear natural frequency of an annular circular plate in contact with a fluid for SS boundary conditions.

In Figures 9 and 10, the change in fluid height on dimensionless nonlinear natural frequency for both CC and SS modes has been investigated.

As shown in Figures 9 and 10, the dimensionless nonlinear natural frequency first increases by increasing fluid height, and tends to be a constant

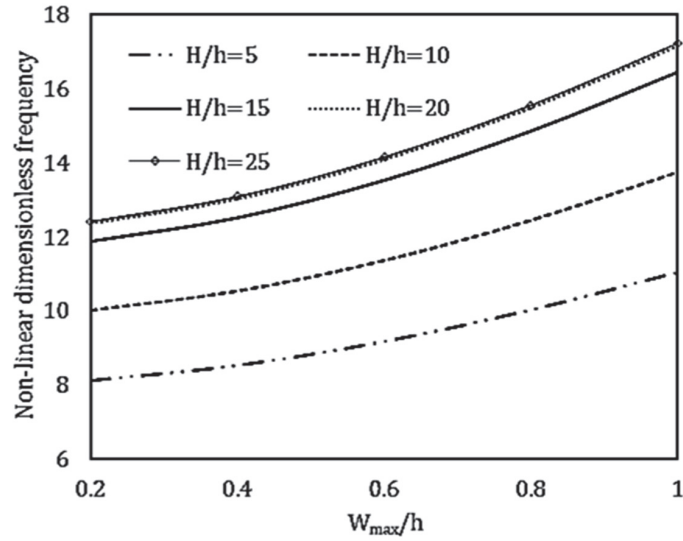


Figure 9 The effect of fluid height on the dimensionless nonlinear natural frequency of an annular circular plate in contact with a fluid for CC boundary conditions.

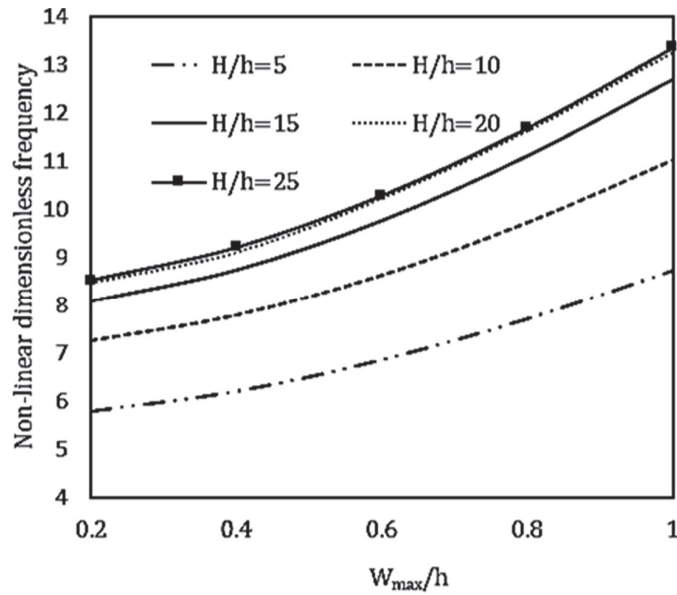


Figure 10 The effect of fluid height on the dimensionless nonlinear natural frequency of an annular circular plate in contact with a fluid for SS boundary conditions.

value. Further, an increase in the height can have a slight effect on the dimensionless frequency, which indicates that the fluid with more depth affects the vibrational behavior of the circular plate slightly. With the onset of vibrational motion, the wave created by the vibration enters the fluid, is propagated in, strikes the lower rigid plane, and is created as the opposite wave in the fluid and causes opposition to the vibrating motion of the plate and thus reduces the frequency. This phenomenon is significant at low fluid height, but by increasing height there is not enough time to reach opposite waves to the vibration of the plate, and deeper fluid can have less impact on this phenomenon.

6 Conclusion

In this study, the effect of the presence of a fluid on the nonlinear natural frequency has been investigated. The dynamic pressure from the fluid on the plate has been obtained by solving the Laplace equation and applying boundary conditions in terms of transverse displacement of the plate. In addition, the nonlinear differential equations have been determined based on the solved DQ method. Then, the effect of various parameters such as dimensional ratios, fluid density, and fluid height on the nonlinear natural frequency has been evaluated. Further, the results obtained without considering the fluid have been validated by comparing to those of the previous studies, which indicated a good convergence. The following results have been presented for all boundary conditions:

- The nonlinear natural frequency increases by increasing the a / b ratio (decreasing the width of the circular plate).
- The nonlinear natural frequency increases by increasing h / b ratio (thickening of the plate).
- The nonlinear natural frequency decreases when the fluid density increases. Additionally, the natural frequency of the plate decreases with a very steep slope in the range of density changes from 0 to 0.3, which indicates that the presence of fluid reduces the nonlinear natural frequency significantly.
- An increase in the fluid height leads to an increase in the nonlinear natural frequency, and then tends to become a constant value. In addition, an increase in height can slightly affect the natural frequency, which indicates that the distant fluid has little effect on the vibrational behavior of the circular plate.

Funding

This research received no specific grant from any funding agency in the public, commercial, or not-for-profit sectors.

Conflict of Interest

The authors declare no conflict of interest in preparing this article.

References

- [1] Kwak, M. K., & Kim, K. C. (1991). Axisymmetric vibration of circular plates in contact with fluid. *Journal of Sound and Vibration*, 146(3), 381–389. [https://doi.org/10.1016/0022-460X\(91\)90696-H](https://doi.org/10.1016/0022-460X(91)90696-H)
- [2] Endo, H. (2000). The behavior of a VLFS and an airplane during take-off/landing run in wave condition. *Marine structures*, 13(4–5), 477–491. [https://doi.org/10.1016/S0951-8339\(00\)00020-4](https://doi.org/10.1016/S0951-8339(00)00020-4)
- [3] Kozlovsky, Y. (2009). Vibration of plates in contact with viscous fluid: Extension of Lamb's model. *Journal of Sound and Vibration*, 326(1–2), 332–339. <https://doi.org/10.1016/j.jsv.2009.04.031>
- [4] Askari, E., Jeong, K. H., & Amabili, M. (2013). Hydroelastic vibration of circular plates immersed in a liquid-filled container with free surface. *Journal of sound and vibration*, 332(12), 3064–3085. <https://doi.org/10.1016/j.jsv.2013.01.007>
- [5] Tariverdilo, S., Shahmardani, M., Mirzapour, J., & Shabani, R. (2013). Asymmetric free vibration of circular plate in contact with incompressible fluid. *Applied Mathematical Modelling*, 37(1–2), 228–239. <https://doi.org/10.1016/j.apm.2012.02.025>
- [6] Allahverdizadeh, A., Naei, M. H., & Bahrami, M. N. (2008). Nonlinear free and forced vibration analysis of thin circular functionally graded plates. *Journal of sound and vibration*, 310(4–5), 966–984. <https://doi.org/10.1016/j.jsv.2007.08.011>
- [7] Jeong, K. H. (2003). Free vibration of two identical circular plates coupled with bounded fluid. *Journal of Sound and Vibration*, 260(4), 653–670. [https://doi.org/10.1016/S0022-460X\(02\)01012-X](https://doi.org/10.1016/S0022-460X(02)01012-X)
- [8] Jeong, K. H., & Kim, K. J. (2005). Hydroelastic vibration of a circular plate submerged in a bounded compressible fluid. *Journal of Sound and Vibration*, 283(1–2), 153–172. <https://doi.org/10.1016/j.jsv.2004.04.029>

- [9] Amabili, M. (1996). Effect of finite fluid depth on the hydroelastic vibrations of circular and annular plates. *Journal of Sound and Vibration*, 193(4), 909–925. <https://doi.org/10.1006/jsvi.1996.0322>
- [10] Shafiee, A. A., Daneshmand, F., Askari, E., & Mahzoon, M. (2014). Dynamic behavior of a functionally graded plate resting on Winkler elastic foundation and in contact with fluid. *Struct. Eng. Mech*, 50(1), 53–71. <http://dx.doi.org/10.12989/sem.2014.50.1.053>
- [11] Canales, F. G., & Mantari, J. L. (2017). Laminated composite plates in contact with a bounded fluid: Free vibration analysis via unified formulation. *Composite Structures*, 162, 374–387. <https://doi.org/10.1016/j.compstruct.2016.11.079>
- [12] Bo, J. (1999). The vertical vibration of an elastic circular plate on a fluid-saturated porous half space. *International journal of engineering science*, 37(3), 379–393. [https://doi.org/10.1016/S0020-7225\(98\)00073-1](https://doi.org/10.1016/S0020-7225(98)00073-1)
- [13] Khorshidi, K., Akbari, F., & Ghadirian, H. (2017). Experimental and analytical modal studies of vibrating rectangular plates in contact with a bounded fluid. *Ocean Engineering*, 140, 146–154. <https://doi.org/10.1016/j.oceaneng.2017.05.017>
- [14] Soni, S., Jain, N. K., & Joshi, P. V. (2018). Vibration analysis of partially cracked plate submerged in fluid. *Journal of Sound and Vibration*, 412, 28–57. <https://doi.org/10.1016/j.jsv.2017.09.016>
- [15] Soni, S., Jain, N. K., & Joshi, P. V. (2019). Stability and dynamic analysis of partially cracked thin orthotropic microplates under thermal environment: An analytical approach. *Mechanics Based Design of Structures and Machines*, 1–27. <https://doi.org/10.1080/15397734.2019.1620613>
- [16] Jomehzadeh, E., Saidi, A. R., & Atashipour, S. R. (2009). An analytical approach for stress analysis of functionally graded annular sector plates. *Materials & design*, 30(9), 3679–3685. <https://doi.org/10.1016/j.matdes.2009.02.011>
- [17] Hejripour, F., & Saidi, A. R. (2012). Nonlinear free vibration analysis of annular sector plates using differential quadrature method. *Proceedings of the Institution of Mechanical Engineers, Part C: Journal of Mechanical Engineering Science*, 226(2), 485–497. <https://doi.org/10.1177/0954406211414517>
- [18] Canales, F. G., & Mantari, J. L. (2017). Laminated composite plates in contact with a bounded fluid: Free vibration analysis via unified formulation. *Composite Structures*, 162, 374–387. <https://doi.org/10.1016/j.compstruct.2016.11.079>

- [19] Bert, C. W., & Malik, M. (1996). Differential quadrature method in computational mechanics: a review. <https://doi.org/10.1115/1.3101882>
- [20] Malekzadeh, P. (2007). A differential quadrature nonlinear free vibration analysis of laminated composite skew thin plates. *Thin-walled structures*, 45(2), 237–250. <https://doi.org/10.1016/j.tws.2007.01.011>
- [21] Amini, M. H., Soleimani, M., Altafi, A., & Rastgoo, A. (2013). Effects of geometric nonlinearity on free and forced vibration analysis of moderately thick annular functionally graded plate. *Mechanics of Advanced Materials and Structures*, 20(9), 709–720. <https://doi.org/10.1080/15376494.2012.676711>

Biographies



Amir Hossein Nasrollah Barati is Ph.D. student in Mechanical Engineering department in the Science and Research Branch of the Islamic Azad university, Tehran, Iran. His research interests include Nonlinear Dynamics, Mechanical Vibration, and Solid-Fluid interaction.



Ali Asghar Jafari is Professor in K. N. Toosi University of Technology, Tehran, Iran. His research interests Dynamics and Computational Mechanics,

Numerical Methods in Engineering, Solid-Fluid interaction, Mechanical Vibration.



Shahram Etemadi Haghighi is Assistant Professor in Mechanical Engineering department in the Science and Research Branch of the Islamic Azad university, Tehran, Iran. His research interests include Nonlinear Systems and Control.



Adel Maghsoudpour is Assistant Professor in Mechanical Engineering department in the Science and Research Branch of the Islamic Azad university, Tehran, Iran. His research interests Mechanical Vibration and Control.